Molecular Crystals and Liquid Crystals
Publication details, including instructions for authors and subscription information:
http://www.tandfonline.com/loi/gmcl16

Investigation of NLC Director Orientational Deformations in Electric Field for Different Boundary Conditions

M. I. Barnik [a] , L. M. Blinov [a] , T. V. Korkishko [a] , B. A. Umansky [a] & V. G. Chigrinov [a]
[a] Moscow intermediates and Dyes Institute, 103787, Moscow, B. Sadovaya, 1, USSR
Version of record first published: 17 Oct 2011.

To cite this article: M. I. Barnik , L. M. Blinov , T. V. Korkishko , B. A. Umansky & V. G. Chigrinov (1983): Investigation of NLC Director Orientational Deformations in Electric Field for Different Boundary Conditions, Molecular Crystals and Liquid Crystals, 99:1, 53-79

To link to this article: http://dx.doi.org/10.1080/00268948308072028

Mol. Cryst. Liq. Cryst., 1983, Vol. 99, pp. 53–79
0026-8941/83/9904–053/$18.50/0

Printed in the United States of America

Investigation of NLC Director Orientational Deformations in Electric Field for Different Boundary Conditions†

M. I. BARNIK, L. M. BLINOV, T. V. KORKISHKO, B. A. UMANSKY and V. G. CHIGRINOV

Moscow Intermediates and Dyes Institute, 103787, Moscow, USSR, B. Sadovaya, 1

(Received December 9, 1982)

The work investigates certain director orientational deformations and the corresponding NLC optical characteristics in electric field for different boundary conditions and consists of two Parts.

In Part I we study the effect of Total Internal Reflection (TIR) in NLC layer with homeotropic (B-effect) or planar (S-effect) initial orientation subjected to an external electric field. Strong anchoring of the NLC molecules with the substrates is assumed. The intensity of the transmitted light vs angle of incidence is shown to exhibit very sharp and deep oscillations in the vicinity of the TIR angle, the period and the amplitude of the oscillations depending on the applied voltage. The calculated TIR values in B- and S-effects agree with our experimental data.

In Part II we investigate orientational deformations of homeotropically aligned NLC layer in an electric field parallel and perpendicular to the initial director orientation (B-effect and flexoeffect respectively). The apparent strong anchoring of the NLC molecules with the substrates in B-effect, found in our experiment, is explained by introducing the surface energy coupling in the new form.

The director of a nematic liquid crystal (NLC) orients in an electric field in accord with the condition of the torques balance, so that the dielectric torque, which is proportional to $\varepsilon_a E^2$ (ε_a is the NLC dielectric anisotropy, E is the applied electric field) becomes equal to the elastic torque, tending to return the NLC director to its initial arrangements.‡ The value of the

†Presented at the Ninth International Liquid Crystal Conference, Bangalore, 1982.

‡In many cases the volume flexoelectric torque as well as the surface one is to be taken into account.[1]

elastic torque depends on the boundary conditions at the NLC surface and the anchoring energy, characterizing the strength of the NLC molecules attachment to the limiting substrates. The director reorientation in a thin NLC layer results in the variation of its optical properties, for instance, such as the birefringence or the angle of the Total Internal Reflection (TIR).[2] Despite a large number of papers, devoted to both certain NLC optical properties investigations in orientational effects and the physical origin of the effects themselves, some aspects of the considered problem are not absolutely clear. The present work consists of two parts. In the first Part we investigate the influence of the external electric field on the effect of TIR in NLC, having the initial homeotropic (B-effect) or planar (S-effect) director orientation under the condition of a strong anchoring of the NLC molecules with the substrates. In the second part using the experimental data, obtained in the investigations of the homeotropically oriented NLC layer in an electric field (B-effect)[2] and flexoelectric effect)[3] we show, that the anchoring energy W, characterizing the elastic NLC "resistance" to the external disturbances, has a more complicated dependence on the director deviation angle $\theta - \theta_0$ at the substrates, than that proposed by Rapini,[4] which is widely used nowadays:[1,2]

$$W = \frac{W_o}{2} \sin^2 (\theta - \theta_o) \tag{1}$$

I. TOTAL INTERNAL REFLECTION IN NLC

The investigation of TIR-effect in NLCs is of scientific and practical importance. In point of fact, in some cases[5,6] TIR is completely defined by the director distribution within the NLC thin wall boundary layer, having the thickness of the order of the incident light wavelength. In view of this having measured the TIR angle, we obtain the data, concerning the peculiarities of the NLC director orientation in the vicinity of the solid surface[5] and can evaluate the achoring energy of the molecules with the substrate.[6] The effect of TIR may be used in electrooptical applications of NLCs, such as light modulators or deflectors, operating under low controlling voltages.[2]

The optical properties of a thin nematic layer subjected to an electric field were studied[7] for an obliquely incident light. The calculations of the reflection and transmission were carried out by the numerical method, and developed.[8] The method[8] was also applied[9] for calculating the spectra of TIR in case of NLC Poiseuille flow through a cylindric capillary tube. The theory of the approximate calculating of the TIR angle for certain types of the director orientational deformations (such as flexodeformations, etc.)

and the corresponding experimental results were given.[10] Nevertheless, it should be noted that at present the effect of TIR in NLCs, subjected to an external electric field, is not still absolutely clear.

In Part I of the present work, we propose a simple theoretical model of calculating the transmission of a NLC layer in an electric field for an obliquely incident light in S- and B-effects.[2] The anchoring of the NLC molecules with the substrates is assumed to be strong. The results of the calculations are compared with the experiment.

A. THEORY

Optical properties of NLC layer for an obliquely incident light — application to B- and S-effects.

Let us consider a plane, obliquely incident at an angle i to a NLC layer with the thickness of L, wave of a monochromatic light (TM-wave), polarized in the plane of incidence (XZ-plane) $E_L \exp j(K_x X - \omega t)$, where

$$E_L, \qquad K_x = \frac{2\pi}{\lambda} N \sin i \quad \text{and} \quad \omega = \frac{2\pi c}{\lambda}$$

are the amplitude, wave vector and circular wave frequency, λ–wavelength of light, t–time, c–velocity of light, N–glass refractive index (Figure 1a). The NLC director $\eta = \{\sin \theta(Z), O, \cos \theta(Z)\}$ orients on the plane of incidence, resulting in the refractive index dependence on the coordinate Z along the layer normal. In this case the nonzero components of the electromagnetic field are $E_x(Z,t) = Re\{E_x(Z) \exp(-j\omega t)\}$, $H_y(Z,t) = Re \cdot \{H_y(Z) \exp(-j\omega t)\}$, where Re is the real part. The Maxwell equations for the complex amplitudes of the waves, propagating in NLC $E_x(Z)$ and $H_y(Z)$ are reduced to the following system:

$$\frac{\partial E_\alpha}{\partial Z'} = jk(a_{11}E_x + a_{12}H_y)$$

$$\frac{\partial H_y}{\partial Z'} = jk(a_{21}E_x + a_{11}H_y) \tag{2}$$

Here

$$Z' = Z/L, \qquad K = \frac{2\pi L}{\lambda}, \qquad a_{11} = -N \sin i \frac{(n_\parallel^2 - n_\perp^2) \sin \theta \cos \theta}{n_\perp^2 \sin^2 \theta + n_\parallel^2 \cos^2 \theta},$$

$$a_{12} = 1 - \frac{\sin^2 i N^2}{n_\perp^2 \sin^2 \theta + n_\parallel^2 \cos^2 \theta}, \qquad a_{21} = \frac{n_\perp^2 n_\parallel^2}{n_\perp^2 \sin^2 \theta + n_\parallel^2 \cos^2 \theta}$$

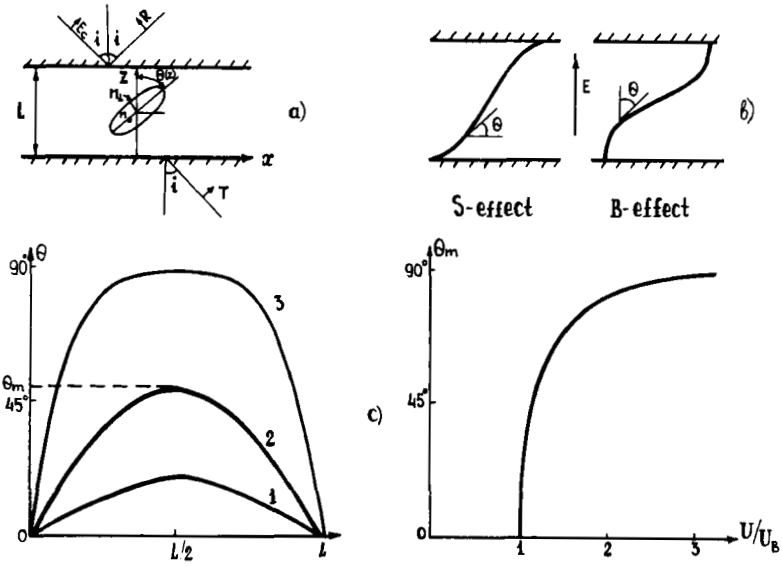

FIGURE 1 (a) A plane monochromatic wave of light with the amplitude of E_L is obliquely incident at an angle i on a NLC cell having the thickness of L. $\theta(z)$ indicates the director orientation along the layer normal; $n_\parallel$ and $n_\perp$ are the main refractive indices parallel and perpendicular to the director respectively; (b) The director distribution $\theta_{S,B}(z)$ in S and B effects; (c) $\theta(z)$ – curves in B-effect for various voltages (MBBA); U/u_B = 1.029(1) 1.211(2), 3.21(3), U_B is the threshold voltage. (d) The corresponding maximum director deviation angle θ_m at the center of the layer vs voltage.

We can rewrite the Eq. 2 in a vector form:

$$\frac{\partial}{\partial Z}\overline{\psi} = jk\hat{A}\overline{\psi} \tag{3}$$

where

$$\overline{\psi} = (E_x, H_y), \qquad A = \begin{pmatrix} a_{11} & a_{12} \\ a_{21} & a_{11} \end{pmatrix}$$

Let us assume below the geometrical optics approximation

$$K = \frac{2\pi L}{\tau} \gg 1 \tag{4}$$

Then the solution of the Eq. 3 up to higher degree terms in powers of K has the form of:

$$\overline{\psi} = \begin{bmatrix} P^{1/2} \exp jk(A + B) & P^{1/2} \exp jk(A + B) \\ P^{-1/2} \exp jk(A + B) & P^{-1/2} \exp jk(A - B) \end{bmatrix} \cdot \begin{bmatrix} C_+ \\ C_- \end{bmatrix}$$

where $C_{\pm} = \text{const.}$, $P(Z') = (a_{12}/a_{21})^{1/2}$,

$$A(Z') = \int_0^{Z'} a_{11}\,dz', \qquad B(Z') = \int_0^{Z'} (a_{12}:a_{21})^{1/2}\,dZ'$$

Taking into account the initial conditions, we have:

$$\overline{\psi} = \hat{F}\overline{\psi}_0$$

where

$$\overline{\psi}_0 = \overline{\psi}(Z' = 0), \qquad \hat{F} = \begin{bmatrix} F_{11} & F_{12} \\ F_{21} & F_{22} \end{bmatrix} \tag{5}$$

$F_{11} = \exp(jkA)\,(P/P_0)^{1/2} \cos KB$, $F_{12} = \exp(jkA) \cdot j \cdot (P_0 \cdot P)^{1/2} \sin KB$, $F_{21} = \exp(jkA) j (P_0 P)^{-1/2} \sin KB$, $F_{22} = \exp(jkA)\,(P_0/P)^{1/2} \cos KB$, $P_0 = P(Z' = 0)$. Wishing to find the amplitudes of the transmitted T and reflected R waves for an oblique incidence of light on the NLC layer we use the method, developed.[8] If T_x, R_x and E_x are the projections of T, R and E on the X-axis, then the vector amplitudes of the transmitted, reflected and incident waves are:

$$\overline{\psi}_t = \begin{pmatrix} T_x \\ r_x T_x \end{pmatrix}, \qquad \overline{\psi}_r = \begin{pmatrix} R_x \\ -r_x R_x \end{pmatrix}, \qquad \overline{\psi}_i = \begin{pmatrix} E_x \\ r_x E_x \end{pmatrix} \tag{6}$$

so that $\overline{\psi}_0 = \overline{\psi}(Z' = 0) = \overline{\psi}_i + \overline{\psi}_r$, $\overline{\psi}_L = \overline{\psi}(Z' = 1) = \overline{\psi}_t$, $z_x = N/\text{cosi}$.

Using Eq. 5 we obtain:

$$\overline{\psi}_t = \hat{F}(\overline{\psi}_i + \overline{\psi}_r) \tag{7}$$

or in the scalar form

$$\begin{aligned} T_x &= F_{11}(E_x + R_x) + F_{12} r_x (E_x - R_x) \\ r_x T_x &= F_{21}(E_x + R_x) + F_{22} r_x (E_x - R_x) \end{aligned} \tag{8}$$

According to Eq. 8 the intensities of the reflected I_r and transmitted I_t waves are:

$$\begin{aligned} I_r &= \frac{R_x}{E_x} = \left| \frac{r_x(F_{22} - F_{11}) + r_x F_{22} - r_x^2 F_{12}}{r_x(F_{11} + F_{22}) - r_x^2 F_{12} - F_{21}} \right|^2 \\ I_t &= \frac{T_x}{E_x} = \left| \frac{2r_x}{r_x(F_{11} + F_{22}) - r_x^2 F_{12} - F_{21}} \right|^2 \end{aligned} \tag{9}$$

where we use the relation $|\det \hat{F}| = |F_{11}F_{22} - F_{12}F_{21}| = 1$, followed from the energy conservation law.

The director distributions in NLC layer, subjected to an external electric field in S- and B-effects are shown on Figure 1b. The effects arise under

the voltages above certain threshold values ($U > U_B = \pi(4\pi K_{33}/-\varepsilon_a)^{1/2}$ in B-effect ($\varepsilon_a < 0$) and $U > U_S = \pi(4\pi K_{11}/\varepsilon_a)^{1/2}$ in S-effect ($\varepsilon_a > 0$). If we assume strong anchoring conditions at the boundaries*, then the director deviation angle $\theta(Z)$ in B- and S-effects becomes a function of NLC parameters only $\chi = K_{11}/K_{33} - 1$ and $\gamma = \varepsilon_\perp/\varepsilon_\parallel - 1$, where K_{11} and K_{33} are the splay and bend elasticity coefficients respectively, $\varepsilon_\parallel$ and $\varepsilon_\perp$—dielectric permittivities along and perpendicular to the director ($\varepsilon_a = \varepsilon_\parallel - \varepsilon_\perp$):[1,2]

$$\theta = \theta_{S,B}(Z', \chi, \gamma, U/U_{S,B}), \tag{10}$$

so that $\theta_{S,B} = 0$ for $Z' = 0, 1$ (Figure 1b). The typical $\theta(Z')$-curves for various voltages are shown on Figure 1c.

Substituting Eq. 10 into Eq. 9 for $Z' = 1$ we calculate the transmittance of the NLC layer subjected to an electric field in B- and S-effects for an oblique incidence of light at an angle i. If $N > \min(n_\perp, n_\parallel)$, then TIR appears at a certain angle $i = i_{\text{TIR}}$.[11] The majority of NLC is characterized by a positive optical anisotropy $\Delta n = n_\parallel - n > 0$, so that the TIR angle varies with increasing the applied voltage within the limits: $\arcsin(n_\perp/N) < i_{\text{TIR}} < \arcsin(n_\parallel/N)$.

As it follows from Eq. 5, the light wave is attenuated for $a_{12} < 0$ and propagates without losses if $a_{12} > 0$. The value $a_{12} = 0$ corresponds to the boundary of the layer, the attenuation starts from. According to this, the TIR angle can be estimated as follows:

$$i_{\text{TIR}} = \min i = \arcsin\left(\frac{n_\parallel^2 \cos^2 \bar{\theta} + n_\perp^2 \sin^2 \bar{\theta}}{N^2}\right)^{1/2} \tag{11}$$

$$\{i : a_{12}(i) = 0\}$$

where $\bar{\theta} = \max \theta(Z')$ if $n_\parallel > n_\perp$. It is evident, that $\bar{\theta} = \theta_m$ for B-effect, where θ_m is the angle at the center of the NLC layer, while in S-effect we have $\bar{\theta} = \theta_b$ being the director orientation at the boundaries (Figure 1).

It should be noted that the similar estimation of the TIR angle has been obtained elsewhere[5,6,10] for the director deformations such as $\bar{\theta} = \max \theta(Z') = \theta_b$. The estimation is correct only if the director orientation near the boundary does not change very rapidly:

$$\left|\frac{d^2\theta}{dZ'^2}, \left(\frac{d\theta}{dZ'}\right)^2\right|_{\theta=\beta_b} \ll K^2$$

*The weak anchoring conditions are considered in Part II of the work.

Increasing the voltage in S-effect results in an abrupt change of the orientation within the boundary layer $(d\theta/dZ')_{\theta=\theta_B} \sim 1$, so that the i_{TIR} estimation by (11) becomes more inaccurate. On the contrary in B-effect the director orientation at the center of the layer is smooth:

$$\left.\frac{d\theta}{dZ'}\right|_{\theta=\theta_m} \equiv 0 \quad \text{and} \quad \left.\frac{d^2\theta}{dZ'^2}\right|_{\theta=\theta_m} \to 0$$

with rising the voltage $[\theta_m \to (\pi/2)]$, thus reducing the error of the estimation (11).

The calculated intensity of the transmitted light wave I_t vs the angle of incidence in B-effect is given in Figure 2. If $i \to i_{TIR} - 0$ and $U \leq U_B$ the transmittance curve exhibits very sharp and deep oscillations so that, the amplitude of the oscillations increases $(I_{t\,max} - I_{t\,min} \sim 1)$ when approaching the TIR angle. The intensity of the reflected wave $I_r(i)$ oscillates in a similar way as it follows from the energy conservation law for nonabsorbing NLCs: $I_r + I_t = 1$.[11] These oscillations arise due to the interference of the light beams reflected from the upper $(z' = 1)$ and lower

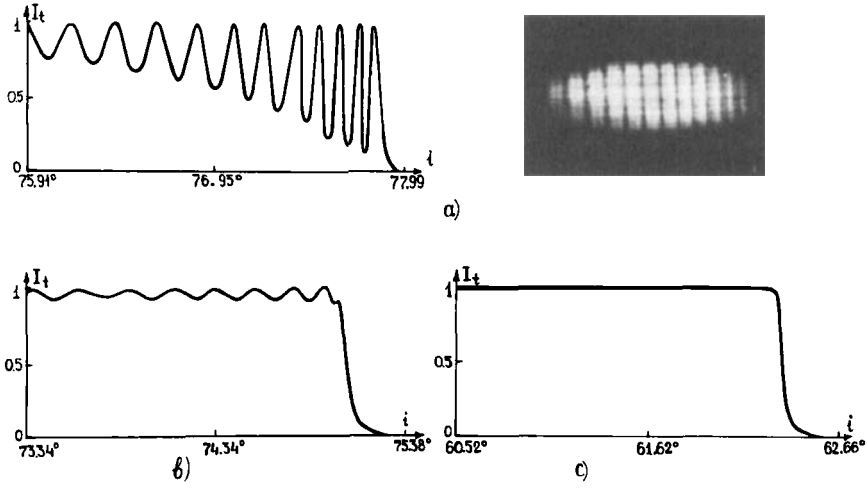

FIGURE 2 The intensity of the transmitted wave I_t vs angle of incidence i in the vicinity of the TIR angle $i \to i_{TIR}$ with increasing the applied voltage in B-effect: $U/U_B = 1$(a), 1.025(b), 1.52(c). We used in the numeric calculations the following NLC parameters (MBBA): $K_{11} = 0.67 \cdot 10^{-6}$ dyne, $K_{33} = 0.83 \cdot 10^{-6}$ dyne, $\varepsilon_\perp = 5.25$, $\varepsilon_\parallel = 4.7$, $n_\parallel = 1.76$, $n_\perp = 1.57$. The flint glass refractive index $N = 1.8$, NLC thickness $L = 22\mu$, wavelength of the incident light $\lambda = 0.63\mu$. The photograph, illustrating the oscillation behavior of the transmitted wave intensity curve at the incidence angles i close to i_{TIR} : $i_{TIR} - 1.5° \leq i \leq i_{TIR}$ for $U/U_B = 0$ is given on the right upper corner of the figure.

($Z' = 0$) boundaries of a thin NLC layer. In the vicinity of the TIR angle $i \to i_{TIR}$ the amplitude of the oscillations increases due to the rising reflection. Let us note, that for $L \geqslant \lambda$ the oscillations of the reflected wave intensity have been also observed in thin isotropic films.[12,13]

Assuming in (2) $n_\perp = n_\parallel = n$ one can obtain the following approximate formula for I_t when $i \to i_{TIR}$:

$$I_t \sim \frac{8N^4}{n^3(N^2 - n^2)^{1/2}} \cdot \frac{\delta_i}{\sin^2\left[\frac{2\pi L}{\lambda}(2n(N^2 - n^2)^{1/2})^{1/2}\,\delta_i^{1/2}\right]} \tag{12}$$

where $0 < \delta_i = i_{TIR} - i \ll 1$. The number of the intensity maxima

$$M \sim \frac{2L}{\lambda}\sqrt{2n(N^2 - n^2)^{1/2}}\,\delta_i^{1/2} \tag{13}$$

is in a qualitative agreement with the results of the calculations (Figure 2): for $\delta_i \sim 0.02$ we have $M \sim 15$.

The sharp intensity oscillations of the reflected from the NLC layer light wave in the vicinity of the TIR angle seem to have been observed for the first time in[9] for Poiseuille flow of NLC through a cylindric capillary tube. In this case the function $I_r(i)$, $i \to i_{TIR}$ depends on the director distribution on the plane of the light incidence. In B-effect the intensity of the transmitted wave is a function of the applied field. When the applied voltage U exceeds the threshold value U_B, the amplitudes of the oscillations fall down, while the distance between the maxima increases so that at a certain voltage $I_r(i)$ takes the form of a step function, as in TIR from a semi-infinite medium.[11] This effect seems to take place due to the decrease with increasing the voltage of the thickness $L = L_{eff}$ of the effective layer, in which the propagating waves do not attenuate. The interfering light beams are reflected from the boundaries of this layer. The transformations of the intensity curve may be qualitatively explained by substituting into Eq. 12 the decreasing values of L. As it follows from Eq. 5 the effective layer extends to the values of Z' for which $a_{12} \geqslant 0$. The effective layer in B-effect is located near the NLC layer boundaries (Figure 1b).

The TIR-phenomenon in S-effect has its peculiarities, though, from the formal point of view, the relations Eqs. 9–10 remain the same, if one changes $\theta \to (\pi/2) - \theta$ (Figure 1b) or (which is an equal operation) $n_\perp \rightleftarrows n_\parallel$, $K_{11} \rightleftarrows K_{33}$, $\varepsilon_\perp \rightleftarrows \varepsilon_\parallel$. In S-effect the light, incident at an angle i_{TIR}, penetrates into the NLC layer only over the distance of the order of the light wavelength $\lambda \ll L$.[11] The penetration depth varies very slowly with increasing the voltage. The behavior of the transmitted wave intensity $I_t(i)$ in S-effect differs from that one in B-effect. As it is shown in Figure 3 the

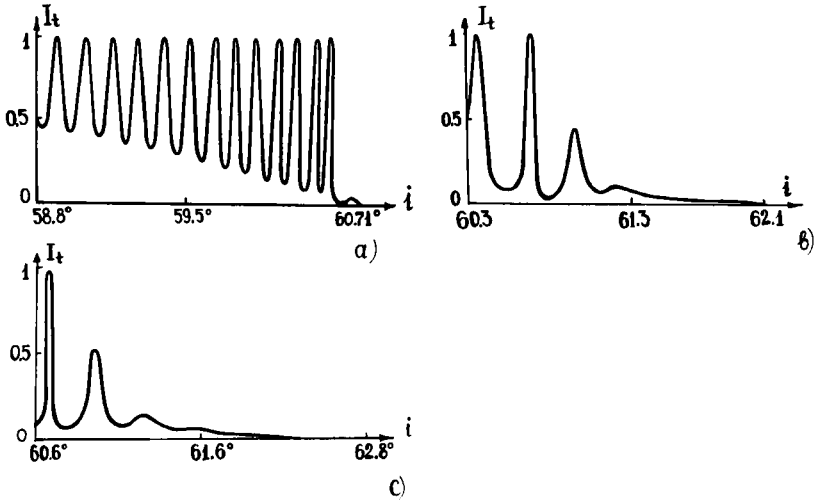

FIGURE 3 The transmitted wave intensity I_t vs angle of incidence i in the vicinity of the TIR angle $i \rightarrow i_{TIR}$ with increasing the applied voltage in S-effect: U/U_S = 1.027(a), 2.616(b), 3.098(c), U_S–is the threshold voltage of S-effect. We used in the numeric calculations the parameters of MBBA as in Figure 2 except the value $\varepsilon_\parallel = 5.35$.

curve $I_t(i)$ in S-effect is of an oscillating character even for $U \gg U_s$. It should be also noted, that when $i \rightarrow i_{TIR}$ the transmittance $I_t(i)$ is tending to zero very slowly, which gives an appreciable error in the definition of the i_{TIR} angle. The oscillations on the transmitted wave intensity curve $I_t(i)$ when $i \rightarrow i_{TIR}$, observed even for very high voltages, may be explained by the fact, that in S-effect the effective layer ($a_{12} \geqslant 0$) extends to almost all the NLC thickness except small boundary regions.

Experimental results — comparison with the theory

The investigation of B-effect were carried out using MBBA at room temperatures. The elastic moduli of MBBA are $K_{11} = 0.67 \cdot 10^{-6}$ dyne and $K_{33} = 0.83 \cdot 10^{-6}$, the refractive indices $n_\parallel = 1.76$ and $n_\perp = 1.57$ (at the wavelength $\lambda = 632.8$ nm) and the dielectric anisotropy $\varepsilon_a = \varepsilon_\parallel - \varepsilon_\perp = -0.55$. The TIR phenomenon in S-effect was investigated in MBBA, doped with n-cyanophenyl ester of n-heptylbenzoic acid (CEHBA). The dielectric anisotropy of the doped MBBA was $\varepsilon_a = +0.1$, the other parameters being practically the same as in pure MBBA.[14]

The liquid crystal was placed between two flint-glass cylindric lenses (the refractive index $N = 1.8$), which inner surfaces were coated with SnO_2 transparent electrodes. The NLC thickness $L = 22\mu$ was fixed by teflon

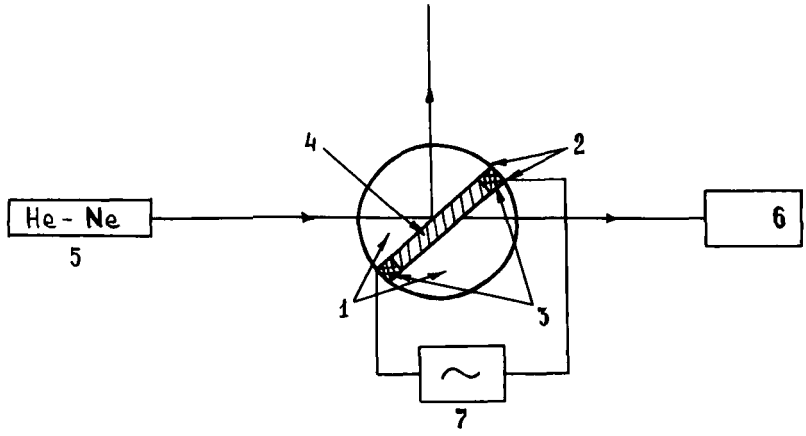

FIGURE 4 The experimental set-up for the TIR angle measurements. (1) Flint-glass cylindrical lenses; (2) SnO_2 transparent electrodes; (3) Teflon spacers; (4) NLC; (5) He-Ne-laser; (6) Photomultiplier; (7) D. C. generator.

spacers. The initial planar orientation for S-effect observations was made by rubbing the electrodes, preliminarily coated with a thin film of a polyvinyl alcohol. To observe B-effect the initial homeotropic orientation was made by treating the lenses surfaces with a stearinchloride of chromium.

The experimental set up is given on Figure 4. A polarized He–Ne (λ = 632.8 nm) laser beam perpendicularly incident on the cylindric surface, crossed at a certain angle the NLC layer and, keeping the direction unchanged, got into a photomultiplier or a screen placed behind the NLC cell. The variation of the angle of incidence was made with the help of Fedorov's table, which the NLC-cell was locked on. The TIR angle was defined by the transmitted wave intensity extrapolation to a zero level. The accuracy of the TIR angle measurements was limited by the divergence of the laser beam which was of the order of $10' \div 15'$.

The photograph, which illustrates an oscillating behavior of the reflected wave intensity at incidence angles i close to $i = i_{TIR}$ is given on Figure 2. In this experiment we increased the divergence of the laser light beam up to ~1.5°, using a long-focal-length lens. Thus several interference maxima and minima were observed simultaneously, because the light beam included all the angles of incidence i with the range $i_{TIR} - 1{,}5° \leq i \leq i_{TIR}$.

Figure 5 shows the TIR angle dependence on the applied voltage $U/U_{B,S}$ in B- and S-effects. The dots indicate the experimental values, the solid lines correspond to the i_{TIR}-curves obtained in the computations, using the relations of Eqs. 9 and 10, where i_{TIR} was defined as an angle of incidence, for which $I_t(i_{TIR}) = 10^{-2}$. The dashed line is drawn in accordance with the qualitative estimation Eq. 11, of the TIR angle. The sharp fall of the i_{TIR}

value with rising the applied voltage in B-effect corresponds to the rapid growth of the director deviation angle at the center of the NLC layer $\bar{\theta} = \theta_m(U)$ (Figure 1d). At the same time a slow increase of the TIR angle $i_{TIR}(U)$ in S-effect for strong anchoring conditions ($\bar{\theta} = \theta_b \equiv 0$) is caused by the abrupt change of the NLC orientation within the boundary layer for the sufficiently high values of the applied voltage. As we have already mentioned above, the error of the i_{TIR} estimation by Eq. 11 increases with the voltage in S-effect and the situation is quite the reverse in B-effect (Figure 5). It should be noted once more, that measuring the i_{TIR} values in B-effect one obtains only the data concerning the NLC orientation at the center of the layer.

Thus in Part I of the present work we have investigated the effect of Total Internal Reflection of a NLC layer subjected to an electric field in orien-

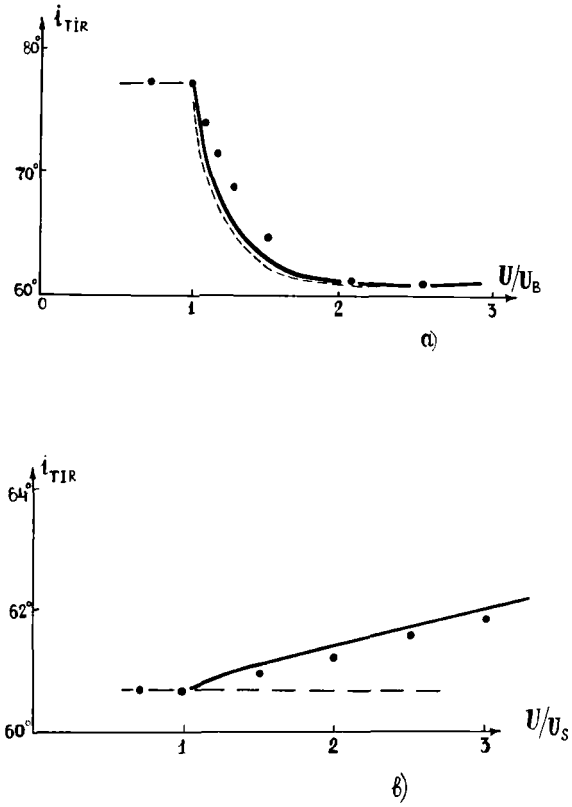

FIGURE 5 The TIR angle i_{TIR} dependence on the applied voltage $U/U_{B,S}$ in B (Figure 5a) and S (Figure 5b) effects. The solid lines indicate our numerical calculations, dots–experimental data, dashed line–the evaluation in accord with (11). $I_r(i_{TIR}) = 10^{-2}$, the other parameters are taken as for Figure 2.

tational *S*- and *B*-effects provided that strong anchoring conditions at the boundaries are fulfilled. In the second part we shall lift the last restriction and consider weak anchoring in the orientational NLC deformations.

II. ORIENTATIONAL DEFORMATIONS IN HOMEOTROPIC NLC LAYERS

New type of boundary conditions

One of the most important Liquid Crystal (LC) characteristics is the anchoring energy of the LC molecules with the limiting boundaries. The term "anchoring energy" ("surface energy coupling", etc.) has been introduced by Rapini and Papoular[4] in the form of Eq. 1. The anchoring strength coefficient $W_o/2$ in Eq. 1 is equal to the energy, needed for the maximum director deviation $\theta - \theta_o$ from the initial orientation θ_o at the boundaries. The anchoring energy W exerts a considerable influence on the equilibrium LC configuration with[15] or without[6,16,17] external disturbances and, besides, defines dynamic[18] and threshold[6,19] characteristics of certain electro and magnetooptical effects. Nehring, *et al.*,[19] have shown, in particular, that taking into account weak boundary coupling results in a considerable dependence of the threshold voltage of an orientational effect U_{th} on the anchoring coefficient W_o and the cell thickness L:[20]

$$\tilde{U}_{th} = U_{th}\left(1 + \frac{2K_{ii}}{LW_o}\right)^{-1} \tag{14}$$

where U_{th} is the threshold voltage provided that strong anchoring conditions $W_o \to \infty$ are fulfilled.*

The variation of the birefringence δ and the director orientations θ_m at the center of the layer and θ_b at its boundaries vs applied voltage are also affected by the value of the anchoring strength coefficient W_o.[19] Weak anchoring of the NLC director with the substrates causes steeper transitions with complete saturation of $\delta(U)$, $\theta_m(U)$ and $\theta_b(U)$ at low electric fields. The typical curves $\delta(U/U_B)$ and $\theta_b(U/U_B)$ in *B*-effect (Figure 1b) are shown on Figure 6.

The threshold voltage dependence on the NLC layer thickness in the form of (14) may be used in "Rapini model" to determine the anchoring coefficient W_o. However, certain measurements of the threshold voltage values show,[21] that these values do not depend on the NLC layer thickness,

*$U_{th} = U_B$ or U_S in S- and B-effects respectively.

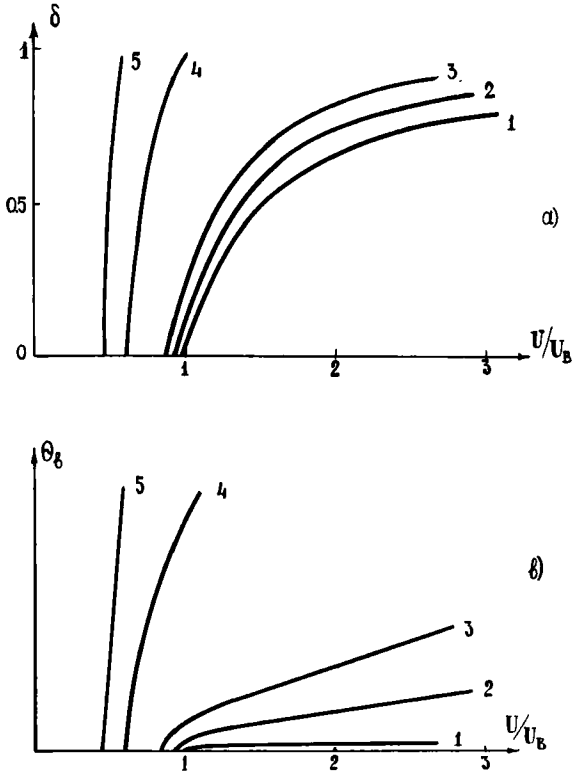

FIGURE 6 The birefringence δ and the director orientation θ_b at the boundaries vs voltage U/U_B in B-effect. The numeric calculations were carried out using the "Rapini model" of anchoring energy (1). The NLC thickness $L = 22\mu$; anchoring coefficient $W_o = 0.1$ erg/sm^2 (curve 1), 0.01(2), 0.005(3), 0.001(4), 0.0005(5).

which, in accordance with (14), entails the strong anchoring conditions ($W_o \geq 0.1$ erg/sm^2). If the initial NLC orientation is planar the strong anchoring is quite acceptable[20] and confirmed in a series of experiments.[1] However, in case of initial homeotropic alignment this degree of anchoring contradicts with a number of measurements with different techniques.[6,17,22] In particular, the flexoeffect in the Helfrich cell geometry,[3] observed in some experiments[23-25] is possible only under weak anchoring conditions. The phase difference $\Delta\Phi$ in flexoeffect:

$$\Delta\Phi = \frac{\Delta\Phi_o}{\left(1 + \frac{LW_o}{2K_{33}}\right)^2}, \qquad \Delta\Phi_o = \frac{\pi \, \mathrm{Ln}_\perp}{12\lambda}\left(1 - \frac{n_\perp^2}{n_\parallel^2}\right)\frac{U^2}{U_H^2}, \qquad (15)$$

is derived using the anchoring energy in the form of Eq. 1, where $\Delta\Phi_o = \Delta\Phi(W_0 = 0)$, $U_H = K_{33}/e_{33} + m_p$, e_{33}–flexocoefficient, m_p–surface polarization, U-external voltage.

The problem of the surface energy coupling and estimation of the anchoring coefficient W_o acquires special significance due to the growing interest in the LC research as a whole and orientational effects in LC, in particular.[1,2] In all the papers, we have come through, the anchoring energy W is invariably taken in the form, proposed by Rapini in Eq. 1. However, in general case, W may be an arbitrary function of the director deviation square value at the boundaries $(\theta - \theta_o)^2$, the expression in Eq. 1 being one of the possible approximations. In Part II of the present work we propose a more general type of the surface energy coupling than that given earlier by Rapini. The validity of our model is confirmed by experimental investigations of certain orientational deformations of homeotropically oriented NLC layer in an electric field.

A. EXPERIMENTAL TECHNIQUE AND RESULTS.

Orientational NLC director deformations were investigated by measuring the phase difference values between ordinary and extraordinary rays, passed through a NLC layer, placed between two parallel glass plates with SnO_2 transparent layers on the inner surfaces. The thickness of the layer was fixed by teflon spacers. The phase difference and the threshold of the deformation were defined using the NLC-cell transmittance-voltage characteristics, registered in crossed polaroids by means of two-coordinate recorder. The velocity of the voltage scanning, applied to the cell was 0.25 mvolt/sec.

In investigation of the flexoeffect we did not coat the glass substrates with the SnO_2 conducting layer, using two parallel aluminum or copper strips both as the electrodes and the spacers. The measurements of the phase difference were carried out by Senarmont compensator, built into a polarizing microscope.

In the experiment we used MBBA, which was oriented homeotropically by depositing a stearinchloride of chromium onto the inner surfaces of the glass plates. The thickness of the empty cell was defined by the interference technique[26] with the accuracy of 5%. The error in measuring the threshold voltage did not exceed 2%. The accuracy of determining the phase difference values by the Senarmont compensator was 5%.

The experimental curves of the phase difference vs applied voltage, measured for different NLC layer thickness in B-effect are given on Figure 7. In this case the phase difference values are:[1]

$$\Delta\Phi = \frac{2\pi L}{\lambda}(n_e - n_o) \tag{16}$$

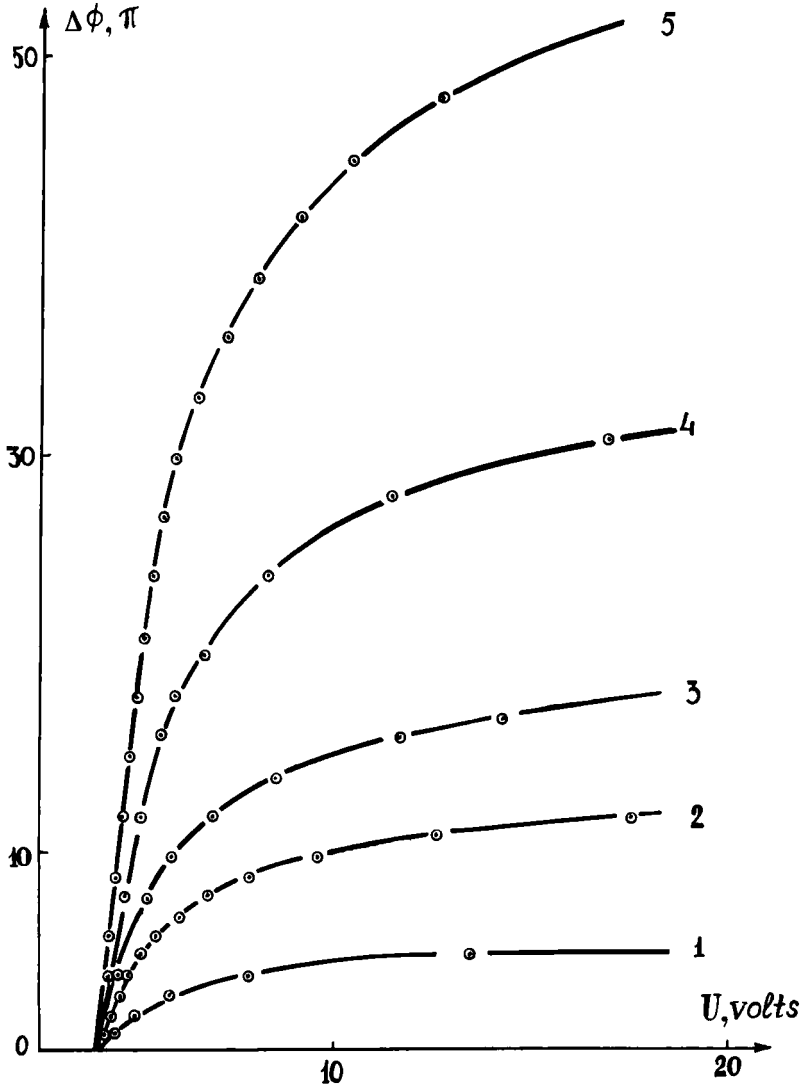

FIGURE 7 Experimental dependences of the phase difference (16) $\Delta\Phi$ vs voltage for different NLC layer thicknesses: $L = 10\mu$ (curve 1), 22(2), 34(3), 60(4), 100(5).

where

$$n_o = n_\perp, \qquad n_e = \frac{1}{L}\int_0^L n(Z)\,dz, \qquad n(Z) = \frac{n_\perp n_\parallel}{(n_\perp^2 \sin^2\theta + n_\parallel^2 \cos^2\theta)^{1/2}}$$

(Figure 1b). Fig. 7 shows that the threshold voltage U_{th} does not depend on the NLC layer thickness, while in accordance with (14) it must reduce in value with decreasing the thickness, which is especially appreciable in case of weak anchoring.* Taking into account the experimental error in definition of the U_{th}-values ~ 2% we can estimate from (14) anchoring coefficient

$$W_o \geqslant 0.1 \text{ erg/cm}^2$$

Figure 8 shows the phase difference in flexoeffect vs square of the applied voltage $\Delta\Phi(U^2)$. In accord with (15) these curves are straight lines, so that the value of $\Delta\Phi/U^2L$ is the function of the NLC parameters and the

*We have measured the threshold voltages U_{th} of B-effect in the NLC layers having the thicknesses L from 5 to 200 microns. However, the pronounced dependence $U_{th}(L)$ has not been found.

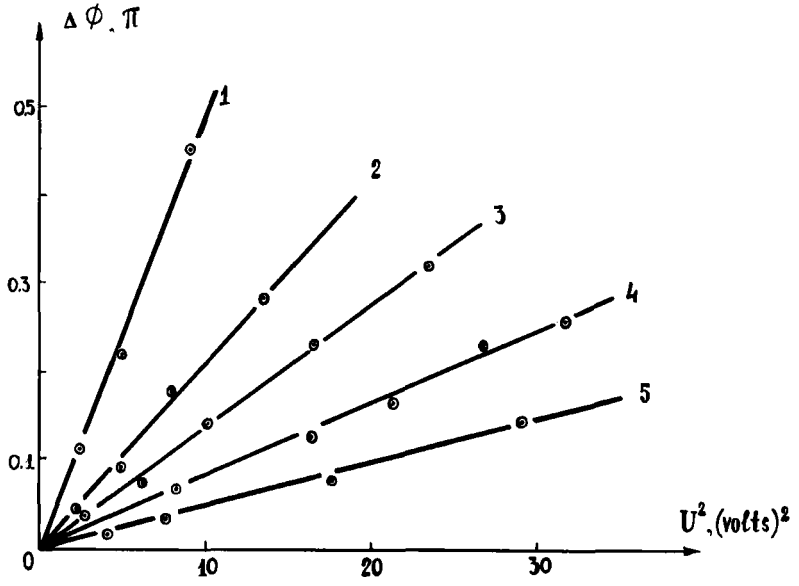

FIGURE 8 The experimental dependences of the phase difference $\Delta\Phi$ (15) in flexoelectric effect vs square of the applied voltage U^2 for the different NLC layer thicknesses L: $L = 100\mu$ (curve 1), 35(2), 20(3), 15(4), 5(5).

anchoring coefficient. Table I gives the $\Delta\Phi/U^2L$ values for the various NLC layer thicknesses, presented on Figure 8. As it is seen from Table I, $\Delta\Phi/U^2L$ values do not depend on L within the limits of the experimental error. Assuming the experimental error to be $\sim 5 \div 10\%$ we come to the conclusion, that the anchoring coefficient, defined from (15) does not exceed $W_o \lesssim 10^{-3}$ erg/cm^2.

Summing up the data we can say, that the anchoring strength coefficient obtained in two different experimental investigations of orientational deformations of the homeotropically aligned NLC layer differs by a factor of 10^2, so that in one case we observe strong anchoring conditions, while another gives quite the opposite result. We shall try to solve the contradiction by introducing the surface energy coupling in the form of the square of the elliptic sinus:

$$W = \frac{W_o}{2}\mathrm{sn}^2(\theta - \theta_o) \tag{17}$$

and consider the above mentioned experimental investigations using this new form of the anchoring energy (17).

B. THEORETICAL CALCULATIONS. COMPARISON WITH EXPERIMENT

Let us consider orientational deformations of the homeotropically aligned NLC layer with the thickness of L in the electric field E. The $\theta(Z)$-values indicate the director deviation angle from the Z-axis (Figure 1a) perpendicular to the substrates. Then the free energy functional F can be written as follows:[1]

$$\begin{aligned} F = \frac{1}{2}\int_0^L \Bigg[& (K_{11}\sin^2\theta + K_{33}\cos^2\theta)\left(\frac{d\theta}{dZ}\right)^2 \\ & + \frac{D_z^2}{4\pi}(\varepsilon_\perp + \varepsilon_a\cos^2\theta)^{-1}\Bigg] dZ \\ & + \left\{\sin\theta\cos\theta\left[(e_{11} + e_{33})E - K_{13}\frac{d\theta}{dZ}\right]\right. \\ & \left. - m_p\cdot\cos\theta\cdot E + W(\theta)\right\}_{Z=L} \\ & + \left\{-\sin\theta\cos\theta\cdot\left[(e_{11} + e_{33})E - K_{13}\frac{d\theta}{dZ}\right]\right. \\ & \left. + m_p\cdot\cos\theta E + W(\theta)\right\}_{Z=0} \end{aligned} \tag{18}$$

TABLE I

NLC layer thickness, microns	100	35	20	15	7
$\Delta\Phi/U^2L \cdot 10^4$, erg^{-1}	2.9	3.4	4,1	3.1	4,1

where e_{11} and e_{33} are flexomoduli, K_{13} is the second order elasticity,[24] m_p–surface polarization,[1] $W(\theta)$–anchoring energy of the NLC director with the substrates, $D_z = (\varepsilon_\perp + \varepsilon_a \cos^2\theta)E$–projection of the electromagnetic induction vector D_z on the Z-axis ($\partial D_z/\partial Z = 0$). Here we suppose both the substrates (at $Z = 0$ and $Z = L$, Figure 1) to be perfectly identical, i.e. characterized by the same anchoring strength coefficient and opposite direction of the surface polarization.

The equilibrium director distribution $\theta(z\,'Z)$ corresponds to the minimum of the functional (18), thus, satisfying the Euler equation:

$$\frac{d^2\theta}{dZ^2}(K_{11}\sin^2\theta + K_{33}\cos^2\theta) + \left(\frac{d\theta}{dZ}\right)^2(K_{11} - K_{33})\sin\theta\cos\theta - \frac{D_Z^2}{8\pi}\frac{\varepsilon_a \sin 2\theta}{(\varepsilon_\perp + \varepsilon_a\cos^2\theta)^2} = 0$$

with the conditions at the boundaries:

$$\left\{\frac{d\theta}{dZ}(K_{11}\sin^2\theta + K_{33}\cos^2\theta) - K_{13}\cos 2\theta\frac{d\theta}{dZ} - K_{13}\sin\theta\cos\theta\frac{d^2\theta}{dZ^2}\left(\frac{d\theta}{dZ}\right)^{-1} + (e_{11} + e_{33})E\sin\theta\cos\theta + m_pE\sin\theta \pm \frac{dW}{d\theta}\right\}_{Z=L,0} = 0 \qquad (20)$$

We consider only "symmetric" solutions*:

$$\theta|_{Z=0} = \theta|_{Z=L}, \qquad \left.\frac{d\theta}{dZ}\right|_{Z=0} = -\left.\frac{d\theta}{dZ}\right|_{Z=L}$$

which correspond to the absolute minimum of the NLC free energy.[1] Then the boundary conditions (20) take the form of:

*For "symmetric" solutions $\left.\frac{d^2\theta}{dZ^2}\right|_{Z=0} = \left.\frac{d^2\theta}{dZ^2}\right|_{Z=L}$.

$$\left\{\frac{d\theta}{dZ}(K_{11}\sin^2\theta + K_{33}\cos^2\theta) - K_{13}\cos 2\theta\frac{d\theta}{dZ} - K_{13}\sin\theta\cos\theta\frac{d^2\theta}{dZ^2}\left(\frac{d\theta}{dZ}\right)^{-1} - \frac{dW}{d\theta}\right\}_{Z=0} = 0 \qquad (21)$$

$$\left.\frac{d\theta}{dZ}\right|_{Z=L/2} = 0 \text{ (the condition of symmetry)}$$

Let us write the potential energy of the NLC director interaction with the substrates in the form of the square of the elliptic sinus (17):

$$W = \frac{W_o}{2}\,\mathrm{sn}^2\,\zeta(\theta) \qquad (22)$$

where $\theta = (\pi/2)[F(\zeta, K)/F(\pi/2, K)]$, $F(\zeta, K) = \int_0^\zeta [d\alpha/(1 - K^2\sin^2\alpha)^{1/2}]$–the elliptic integral of the first kind. The factor K varies within the limits: $0 \le K \le 1$, thus corresponding to the decrease of the "potential gap" halfwidth (Figure 9a) in accord with the expression:

$$L_W \sim \frac{2.59}{\ln[8/(1 - K)]}, \qquad 0 < 1 - K \ll 1 \qquad (23)$$

obtained from (22), if one expands the energy $W(\theta)$ into a power series of the angle θ for $K \to 1$:

$$W \sim \frac{W_o}{2}\left(\theta'^2 - \frac{1 + K^2}{3}\theta'^4\right),$$

$$\theta' = \frac{2}{\pi}F\left(\frac{\pi}{2}, K\right)\theta \sim \frac{1}{\pi}\ln\frac{8}{1 - K}\theta \ll 1 \qquad (24)$$

It should be noted that the value $K = 0$ corresponds to the surface energy potential in the form of Rapini (1), while $K \to 1$ to the infinitely narrow potential gap near the value $\theta = 0$. The value $W_o/2$ remains the height of the potential barrier (Figure 9a).

The director deformation $\theta(z)$ arises only when the external voltage exceeds a certain threshold value U_{th}. In order to find the threshold we assume in (19), (21) $|\theta| \ll 1$, and taking into account (24) write:

$$\frac{d^2\theta}{dZ'^2} + q^2\theta = 0$$

$$\left\{\frac{d\theta}{dZ'}(1 - K_s) - \frac{LW'_o}{K_{33}}\theta\right\}_{Z'=0} = 0$$

$$\left.\frac{d\theta}{dZ'}\right|_{Z'=1/2} = 0 \qquad (25)$$

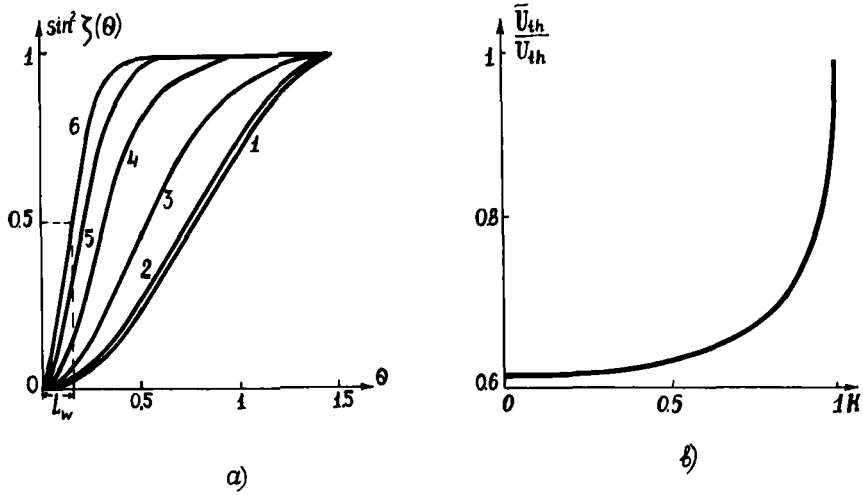

FIGURE 9 (a) The forms of the surface energy coupling (17, 22) for the different values of the factor K: $K = 0$ (curve 1), 0.5(2), 0.95(3), 0.999(4), 0.99999(5), 0.99999999(6). L_w is the halfwidth of the "potential gap". (b) The dependence of the relative threshold $\tilde{U}_{th}/U_{th}$ (27) on the factor K, characterizing the form of the anchoring energy. $L = 22\mu$, $W_o = 10^{-3}$ erg/cm^2. We used in calculations the parameters of MBBA (see Figure 2).

where $Z' = Z/L$, $K_s = K_{13}/K_{33}$, $q^2 = \varepsilon_a U^2/4K_{33}$, $U = EL$, $W_o' \sim (1/\pi)\{\ln]8/(1 - K)]\}^2$–the "effective" anchoring strength coefficient.*

The problem (25) has the solution $\theta = \tilde{A}\cos qZ' + \tilde{B}\sin qZ'$ with the nontrivial coefficients $\tilde{A}$ and $\tilde{B}$ if the following condition is satisfied:

$$\frac{q}{2}\operatorname{tg}\frac{q}{2} = \frac{1}{2}\frac{LW_o'}{K_{33} - K_{13}} \tag{26}$$

coinciding for $K = K_s = 0$ with that one of Rapini.[4] In the limit $LW_o'/(K_{33} - K_{13}) \gg 1$ the expression (26) takes the form $q \sim \pi\{1 - [2(K_{33} - K_{13})]/LW_o'\}$ and the threshold voltage U_{th} is:

$$\tilde{U}_{th} \sim U_{th}\left[1 - \frac{2(K_{33} - K_{13})}{LW_o'}\right] \sim U_{th}\left[1 - \frac{2(K_{33} - K_{13})}{LW_o'} \cdot 1.47 \cdot L_w^2\right] \tag{27}$$

where L_w is the halfwidth of the "potential gap" (23), $U_{th} = U_B$–the threshold voltage of B effect under strong anchoring conditions. Thus it

*For $LW_o'/K_{33} \gg q^2 > 1$ in accord with (25) the term $-K_s\theta\dfrac{d^2\theta}{dZ^2}\left(\dfrac{d\theta}{dZ}\right)^{-1} \sim K_s q^2\dfrac{(K_{33} - K_{13})}{LW_o'}\theta \ll \dfrac{LW_o'}{K_{33}}\theta$ and can be neglected in (25).

follows from (27) that the "effective" anchoring coefficient, obtained from the experiment exceeds the real anchoring coefficient by the factor $W_o'/W_o \sim 1/1.47L_w^2$, which for $K = 0.99999999$, $K_s = 0$ gives $W_o'/W_o \sim 60$. If the apparent anchoring strength coefficient, defined from the experiment $W_o' \geqslant 0.1$ erg/sm^2, then the real one is $W_o \sim 1.7 \cdot 10^{-3}$ erg/sm^2. The estimation (27) of the threshold voltage agrees with the results of our numeric computations (Figure 9b).

The exact solution of the problem (19) and (21) is given by the relation:

$$2Z' \int_{\theta b}^{\theta m} f_1(x)\,dx = \int_{\theta b}^{\theta} f_1(x)\,dx, \qquad \theta(1 - Z') = \theta(Z') \tag{28}$$

where $f_1(x) = (1 + \gamma \sin^2 x)^{1/2}(1 + \chi \sin^2 x)^{1/2}(\sin^2 \theta_m - \sin^2 x)^{-1/2}$

$$\gamma = \frac{\varepsilon_\perp}{\varepsilon_\parallel} - 1, \qquad \chi = \frac{K_{11}}{K_{33}} - 1$$

The director angle at the boundaries:

$$\theta_b = \theta|_{Z'=0} = \theta|_{Z'=1}$$

and at the center of the layer

$$\theta_m = \theta|_{Z'=1/2}$$

depends on the applied voltage U in the following way:

$$\frac{U}{U_B} = \frac{2}{\pi}(1 + \sin^2 \theta_m)^{1/2} \int_{\theta b}^{\theta m} f_2(x)\,dx$$

$$f_2(x) = (1 + \chi \sin^2 x)^{1/2}(1 + \gamma \sin^2 x)^{-1/2}(\sin^2 \theta_m - \sin^2 x)^{-1/2}$$

$$\left[\int_{\theta b}^{\theta m} f_1(x)\,dx/f_1(\theta_b)\right]\left\{\chi \sin^2 \theta_b + 1 - K_s \cos 2\theta_b + K_s \sin^2 \theta_b \cos^2 \theta_b \times (\chi \sin^2 \theta_b + 1)^{-1}\left[\chi + \frac{(1 + \gamma \sin^2 \theta_m)(1 + \chi \sin^2 \theta_b)}{(1 + \gamma \sin^2 \theta_b)(\sin^2 \theta_m - \sin^2 \theta_b)}\right]\right\}$$

$$- \frac{LW_o}{K_{33}} \sin \zeta_b \cos \zeta_b (1 - K^2 \sin^2 \zeta_b)^{1/2} F(\pi/2, k)/\pi = 0 \tag{29}$$

where $K_s = K_{13}/K_{33}$, $\zeta_b = \zeta(\theta = \theta_b)$ is defined from (22). In deriving (29) we have used the following relations:

$$\frac{d\theta}{dz'} = 2 \int_{\theta b}^{\theta m} f_1(x)\,dx/f_1(\theta)$$

$$\frac{d^2\theta}{dZ'^2} = -(\chi \sin^2 \theta + 1)^{-1} \cdot \sin \theta \cos \theta$$

$$\cdot \left[\chi + \frac{(1 + \gamma \sin^2 \theta_m)(1 + \chi \sin^2 \theta)}{(1 + \gamma \sin^2 \theta)(\sin^2 \theta_m - \sin^2 \theta)}\right]\left(\frac{d\theta}{dZ'}\right)^2 \qquad (30)$$

Using (29) we can calculate the dependence of the director orientation θ_b at the boundaries on the applied voltage U. The results of the computations of $\theta_b(U)$ are given in Figure 6 and Figure 10 for $K = 0$ and $K = 0.99999999$ respectively. These values of the factor K correspond to the different forms of the anchoring energy (curves 1 and 6 in Figure 9).

The relative birefringence of the NLC layer:

$$\delta(U/U_B) = \Delta n(U/U_B)/\Delta n_{\max} \qquad (31)$$

where $\Delta n_{\max} = n_\parallel - n_\perp$–is the maximum optical anisotropy, $\Delta n(U/U_B) = \int_0^1 [n(Z') - n_\perp] dZ'$–birefringence for a given value of the applied voltage $U/U_B > 1$ [see also (16)]. Taking into account (30) we can transform (31) as follows:

$$\delta = \left[\int_{\theta b}^{\theta m} f_3(x)\, dx \Big/ \int_{\theta b}^{\theta m} f_1(x)\, dx - 1\right](n_\parallel/n_\perp - 1)^{-1} \qquad (32)$$

where

$$f_3(x) = \left[\frac{(1 + \gamma \sin^2 x)(1 + \chi \sin^2 x)}{(1 + \nu \sin^2 x)(\sin^2 \theta_m - \sin^2 x)}\right]^{1/2}, \qquad \nu = n_\perp^2/n_\parallel^2 - 1$$

The computed values of $\delta(U/U_B)$ for $K = 0$ and $K = 0.99999999$ are given in Figures 6 and 10 respectively. Figure 10 also shows that the threshold voltage of B-effect is practically independent of the NLC layer thickness or, what is the same, of the anchoring coefficient for the surface energy coupling of the new type (17, 22). This agrees with the results of our experimental investigations of the phase difference vs voltage (Figure 7, 10a) but is considerably different from the results obtained in "Rapini model" (Figure 6).

The new form of the surface energy coupling (17, 22) does not affect the qualitative consideration of the flexoelectric NLC deformations given elsewhere.[23,24] If $\varepsilon_a = 0$, then the director orientation in flexoeffect is

$$\theta(Z) = \frac{U}{U_H}\left(\frac{1}{LW_o'/2K_{33} + 1 - K_s}\right) \cdot Z'$$

and phase difference

$$\Delta\Phi = \frac{\Delta\Phi_o}{(LW_o'/2K_{33} + 1 - K_s)^2}$$

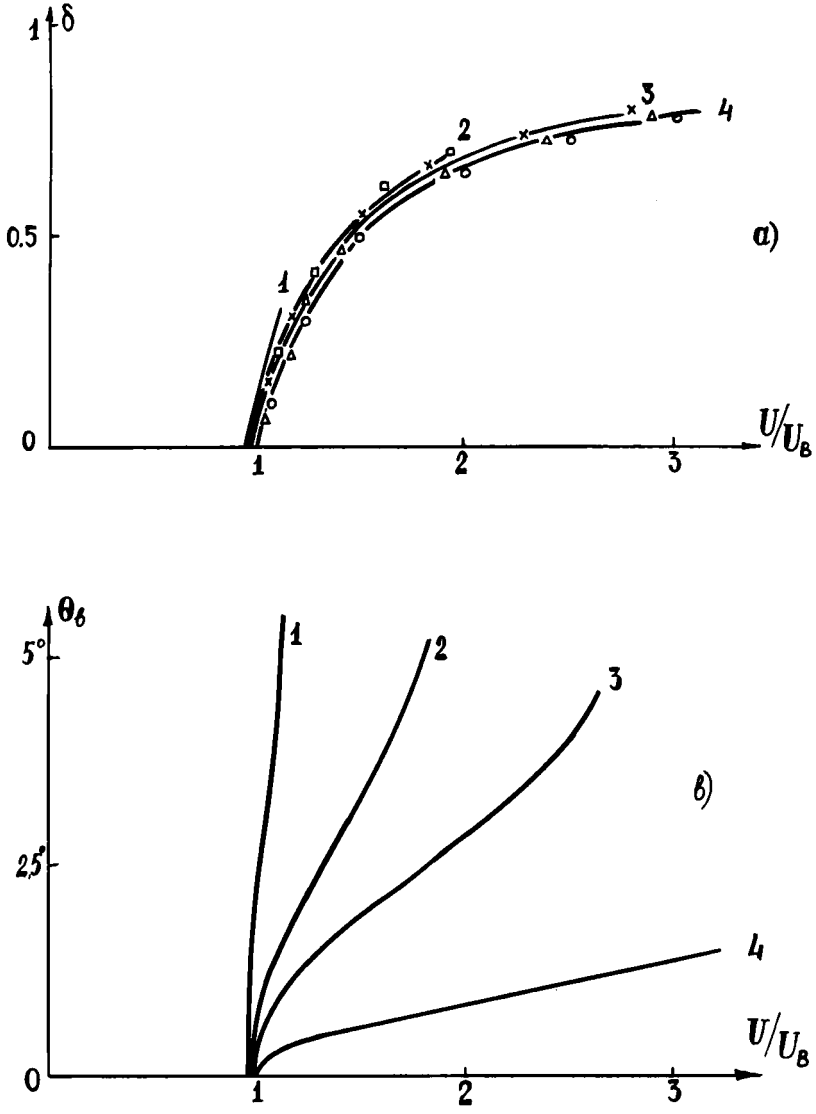

FIGURE 10 The birefringence δ and the director orientation angle θ_b at the boundaries vs voltage in B-effect. The numerical calculations (solid lines) were carried out for the new form of the surface energy coupling (17,22). $W_o = 10^{-3}$ erg/cm^2, $K = 0.99999999$ (curve 6 in Figure 9a). The NLC layer thickness $L = 10\mu$ (curve 1–theory, □–experiment), 22(2, x), 34(3, Δ), 100(4, o).

Here

$$W_o' = W_o\left[\frac{2}{\pi}\cdot F\left(\frac{\pi}{2},K\right)\right]^2 \sim W_o\left(\frac{1}{\pi}\ln\frac{8}{1-K}\right)^2$$

for $K \lesssim 1$ is the "effective" anchoring strength coefficient. In view of this, taking into account the estimation of the anchoring coefficient $W_o' \lesssim 10^{-3}$ erg/cm^2, obtained in our experimental investigation of flexo-effect, we have for the real anchoring $W_o \lesssim 1.7 \cdot 10^{-5}$ erg/sm^2. It should be noted that the difference between two anchoring coefficient values, obtained in our two experiments may be caused by the influence of the SnO_2 conducting layer, which may increase surface energy coupling in B-effect investigations. As it is mentioned above, we have not coated the glass substrates with SnO_2 in the experiment, concerning flexo-deformations. However, we would like to emphasize, that as far as a new type (17, 22) of the surface energy coupling is concerned, the anchoring in both experiments remains weak, contrary to Rapini model.

Let us consider one more aspect of weak anchoring within the framework of our model. As it is shown in Figures 6b and 10b in this case, the director orientation θ_b at the boundaries sharply increases with the voltage and very rapidly approaches the value $\theta_b = \pi/2$. The value of the voltage U_c, the effect is observed at, can be estimated in our model. Assuming, that $\theta \sim \pi/2 - \beta$, $|\beta| \ll 1$ we have from (19):

$$\frac{d^2\beta}{dZ'^2} - S^2\beta = 0, \qquad S^2 = -\frac{\varepsilon_a U^2}{4K_{11}}, \qquad U = EL \tag{33}$$

from which $\beta = AchqZ' + AshqZ'$. The boundary conditions (21) give:

$$\frac{GL}{2K_{11}} = V\left[\text{th } V + 2\frac{K_{13}}{K_{11}}cth(2\cdot V)\right]\cdot A \tag{34}$$

where

$$V = \frac{\pi}{2}\frac{U}{U_s}, \qquad U_s = \pi\sqrt{\frac{4\pi K_{11}}{\varepsilon_a}}$$

The value

$$G = \left.\frac{dW}{d\theta}\right|_{\theta=(\pi/2)-\beta}$$

can be estimated in accordance with (22) as follows:

$$G(K) \sim \left[\frac{2}{\pi}F\left(\frac{\pi}{2},K\right)\sqrt{1-K^2}\right]^2\cdot W_o A \tag{35}$$

As it follows from (35) the equation (34) has no solutions $V \gtrsim \pi/2$ for $K \to 1$. This is confirmed by our computations, which show that for sufficiently low values of W_oL the equations (29) have no solutions, such as $\theta_b = \pi/2$. The solution for θ_b disappears at a certain value of voltage U_c, so that for $U > U_c$ there exists only one solution $\theta_b = \theta \equiv \pi/2$. It means that at $U = U_c$ ($\theta_b = \theta_c$) the director undergoes a discontinuous change to perpendicular with respect to the external field orientation within the whole layer.* For the curves 1 and 2 shown in Figure 10b $U_c = 1.12U_b$, $\theta_c = 0.113$ (in radians) and $U_c = 1.9U_B$, $\theta_c = 0.104$ respectively. The value of $V_c = [(\pi/2)(U_c/U_s)]$ can be estimated from (34), if one notices that in the limit $\beta \sim 1$, when equations (33) and (34) are still correct, the coefficient A in (34) can be found by direct calculations. In point of fact, if we assume in (34):

$$G(K) = \left.\frac{dW}{d\theta}\right|_{\theta=\theta_c} \sim \left.\frac{dW}{d\theta}\right|_{\max} \sim \frac{2\sqrt{2}}{3\pi(1+K^2)^{1/2}} F\left(\frac{\pi}{2}, K\right) W_o \sim \frac{W_o}{3\pi} \ln \frac{8}{1-K}$$

for $k \lesssim 1$,

then the condition $\beta \sim A \sim 1$ gives for $K_{13} = 0$:

$$\frac{GL}{2K_{11}} \sim \frac{W_oL}{6\pi K_{11}} \ln \frac{8}{1-K} = V_c thV_c \sim V_c = \frac{\pi}{2}\frac{U_c}{U_s}$$

$$\text{or} \quad U_c = \frac{W_oL}{K_{11}} \cdot \frac{3}{\pi^2} U_s \ln \frac{8}{1-K} \qquad (36)$$

Finally we would like to find the limits of the second order elasticity K_{13} variations, provided that the surface energy coupling of a new type has taken place. Knowing that $G = (dW/d\theta) > 0$ for any value of $W_o > 0$ we come to the conclusion, that the right side of (34) is also positive. As it follows from this, $K_{13} \geqslant -K_{11} \max_{V \geqslant 0}(thV/2cthV) = -(K_{11}/2)$. In order to find the upper limit for the value of K_{13} we rewrite the equation (34) for the case of S-effect, making the following changes:

$$K_{11} \rightleftarrows K_{33}, \qquad K_{13} \rightleftarrows -K_{13}$$

Then we have:

$$\frac{GL}{2K_{33}} = V\left[thV - \frac{2K_{13}}{K_{33}} cth2V\right] \qquad (37)$$

*If the surface polarization $m_p \neq 0$ then the orientation $\theta \equiv \pi/2$ within the whole NLC layer cannot be achieved (20).

where

$$V = \frac{\pi}{2}\frac{U}{U_B}, \qquad U_B = \pi\sqrt{\frac{4\pi K_{33}}{|\varepsilon_a|}}$$

The positivity of the right side of (37) gives:

$$K_{13} \leq K_{33} \min_{V \geq 0}\left(\frac{thV}{2cth2V}\right) = 0$$

Thus the second order elasticity K_{13} varies within the range:

$$-\frac{K_{11}}{2} \leq K_{13} \leq 0, \tag{38}$$

provided that the surface energy coupling W is an increasing function of the director deviation at the boundaries ($dW/d\theta) > 0$. We have computed the curves $\delta(U/U_B)$ and $\theta_b(U/U_B)$, using the new type of anchoring energy (17, 22) ($k = 0.99999999$) for the value of $K_{13} = -(K_{11}/2)$. The results happen to be only slightly different from those shown in Figure 10. In view of this, as far as a new form of anchoring energy is concerned, one can neglect the elasticity of the second order, assuming $K_{13} = 0$. However, in the case of weak anchoring other factors are to be taken into consideration: a surface flexoelectric torque and a surface polarization [see (20)]. The influence of these parameters on the NLC behavior in orientational effect will be the object of our future investigations.

CONCLUSION

The work investigates certain director orientational deformations and the corresponding NLC optical characteristics in electric field for different boundary conditions and consists of two Parts.

In Part I we study the effect of Total Internal Reflection (TIR) in NLC layer with homeotropic (B-effect) or planar (S-effect) initial orientation subjected to an external electric field. Strong anchoring of the NLC molecules with the substrates is assumed. The intensity of the transmitted light vs angle of incidence is shown to exhibit very sharp and deep oscillations in the vicinity of the TIR angle, the period and the amplitude of the oscillations depending on the applied voltage. The calculated TIR values in B and S-effects agree with our experimental data.

In Part II we investigate orientational deformations of homeotropically aligned NLC layer in an electric field parallel and perpendicular to the initial director orientation (B-effect and flexoeffect respectively). The ap-

parent strong anchoring of the NLC molecules with the substrates in B-effect, found in our experiment, is explained by introducing the surface energy coupling in the new form (17). It should be noted that the expression (17) means only one of the possible approximations of the real form of the surface energy coupling, so that the further theoretical and experimental studies are necessary. Using the experimental curves of the birefringence vs applied voltage for different NLC layer thicknesses we evaluate the anchoring strength coefficient W_o. The value of W_o is in agreement with the results obtained elsewhere:[6,20,22,23]

$$W_o \sim 10^{-3} \div 10^{-5} \text{ erg}/cm^2$$

References

1. V. G. Chigrinov, *Kristallografiya.*, **27**, 404 (1982).
2. L. M. Blinov, Electro and Magnetooptics of liquid crystals, M. Nauka, 1978. English translations: Electrooptical and magnetooptical Properties of Liquid Crystals, J. Wiley & Sons Ltd, Chichester, N. Y. — Brisbane-Toronto-Singapore, 1983.
3. W. Helfrich, *Phys. Letts.*, **A35**, 393 (1971).
4. A. Rapini and M. Papoular, *J. de Phys.*, **30**, Coll. C4, C4–54 (1969).
5. D. Riviere, V. Levy and C. Imbert, *Opt. Communs.*, **25**, 206 (1978); Y. Levy, D. Riviere, C. Imbert and M. Boix, *Opt. Communs.*, **26**, 225 (1978).
6. D. Riviere, Y. Levy and E. Guyon, *J. de Phys. Letts.*, **40**, L–215 (1979); S. Naemura, *Appl. Phys. Letts.*, **33**, 1 (1978).
7. T. Shimomura, H. Mada and S. Kobayashi, *Jap. J. Appl. Phys.*, **15**, 1479 (1976).
8. D. W. Berreman, *J. Opt. Soc. Amer.*, **62**, 502 (1972); **63**, 1374 (1973).
9. D. Riviere and Y. Levy, *Mol. Cryst. Liq. Cryst. Letts.*, **64**, 177 (1981).
10. H. P. Hinov and S. Sainov, *Rev. Phys. Appl.*, **15**, 1307 (1980).
11. M. Born and E. Wolf, "Principles of Optics", Pergamon Press, Oxford, 1968.
12. B. B. Boiko, I. Z. Dgilavdari, G. I. Olefir, N. S. Petrov and V. A. Chernyavskiy, *Kvantovaya electronika*, **7**, 105 (1980).
13. B. B. Boiko, I. Z. Dgilavdari, G. I. Olefir and N. S. Petrov, *Journal priklandnoy spektroskopii*, **30**, 513 (1979).
14. M. I. Barnik, L. M. Blinov, M. F. Grebenkin, S. A. Pikin and V. G. Chigrinov, *Phys. Letts.*, **51A**, 175 (1975).
15. J. Sicart, *J. de Phys. Letts.*, **37**, L–25 (1976).
16. G. Rychenkov and M. Kleman, *J. Chem. Phys.*, **64**, 404 (1976).
17. G. Porte, *J. de Phys.*, **37**, 1245 (1976).
18. H. Yamada and C. Ishii, *Mol. Cryst. Liq. Cryst.*, **76**, 113 (1981).
19. J. Nehring, A. Kmetz and T. Scheffer, *J. Appl. Phys.*, **47**, 850 (1975).
20. E. Guyon and W. Urbach. In. Nonemissive electrooptic displays, New York-London: Plenum Press, 1976, p. 121.
21. M. Ohtsu, T. Akahane and T. Tako, *Jap. J. Appl. Phys.*, **13**, 621 (1974).
22. G. Barbero, R. Malvano and A. Stigazzi, *Nuovo Cimento*, **59B**, 367 (1980).
23. D. Schmidt, M. Schadt and W. Helfrich, *Z. Naturforsch*, **27a**, 277 (1972).
24. A. I. Derzhanski and A. G. Petrov, *Acta Phys. Polon.*, **55A**, 747 (1979).
25. A. I. Chuvyrov, A. S. Sonin and A. D. Zakirova, *Fizika Tverdogo Tela*, **19**, 3084 (1976).
26. L. M. Blinov, V. A. Kizel, V. G. Rumayantsev and V. V. Titov, *J. de Phys.*, **36**, Coll. C1, C1–69 (1975).